Weakly nonlinear optimal disturbances: applications of the theory to the stability of the flow in a micro-channel bound by superhydrophobic walls

Alessandro Bottaro & Jan O. Pralits

Department of Civil, Chemical and Environmental Engineering
University of Genoa, Italy
alessandro.bottaro@unige.it

April 17, 2015

11th ERCOFTAC SIG33 Workshop, St Helier, Jersey, April 15-17, 2015

Experimental, numerical, theoretical activities on SH/LI surfaces at DICCA, Genoa

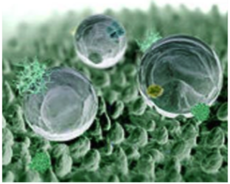

Goals:

- Transition delay (in microfluidic applications)
- Drag reduction (for turbulent flows)

Surface topography

- Micro-ridges (etched onto silicon wafers)
- Hairy surfaces (disordered PDMS pillars obtained through a simple one-step casting technique)
  PDMS=poly(dimethyl)siloxane

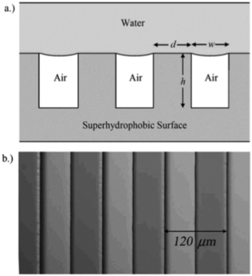

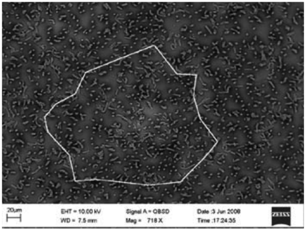

Sponsor: Fincantieri Innovation Challenge, 2014

Slip tensor

The surface texture is accounted for in the velocity boundary condition using a generalization of the Navier condition, the so called **slip tensor** $\boldsymbol{\Lambda}$ introduced by Bazant and Vinogradova (2008).

$$\begin{bmatrix} u(x,\mp 1,z) \\ w(x,\mp 1,z) \end{bmatrix} = \pm \boldsymbol{\Lambda} \frac{\partial}{\partial y} \begin{bmatrix} u(x,\mp 1,z) \\ w(x,\mp 1,z) \end{bmatrix}, \tag{1}$$

where

$$\boldsymbol{\Lambda} = \mathbf{Q} \begin{bmatrix} \lambda^{\parallel} & 0 \\ 0 & \lambda^{\perp} \end{bmatrix} \mathbf{Q}^T, \quad \text{with} \quad \mathbf{Q} = \begin{bmatrix} \cos\theta & -\sin\theta \\ \sin\theta & \cos\theta \end{bmatrix} \tag{2}$$

and $\lambda^{\parallel}$, $\lambda^{\perp}$ are longitudinal and transverse slip lengths.

In particular we consider micro-ridges for which $\lambda^{\parallel} = 2\lambda^{\perp}$ Lauga and Stone (2003); Philip (1972); Belyaev and Vinogradova (2010)

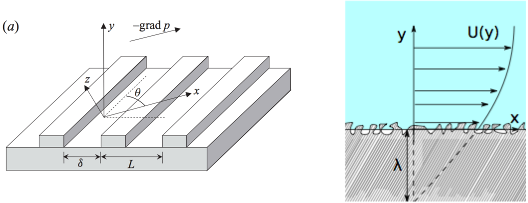

Figure: Definition of the micro-ridges and the coordinate system.

Base flow

The governing equations for plane, incompressible and steady channel flow, read

$$\frac{\partial P}{\partial x} = \frac{1}{Re}\frac{\partial^2 U}{\partial y^2}, \quad V = 0, \quad \frac{\partial^2 W}{\partial y^2} = 0, \qquad \text{and} \qquad Re = \frac{\bar{U}^\star h^\star}{\nu^\star} \tag{3}$$

Analytical solutions, for 2 cases, are found by imposing the following boundary conditions

$$\begin{bmatrix} U(-1) \\ W(-1) \end{bmatrix} = \mathbf{\Lambda}\frac{\partial}{\partial y}\begin{bmatrix} U(-1) \\ W(-1) \end{bmatrix} \qquad \begin{bmatrix} U(\mp 1) \\ W(\mp 1) \end{bmatrix} = \pm\mathbf{\Lambda}\frac{\partial}{\partial y}\begin{bmatrix} U(\mp 1) \\ W(\mp 1) \end{bmatrix}$$

$$U(1) = W(1) = 0$$

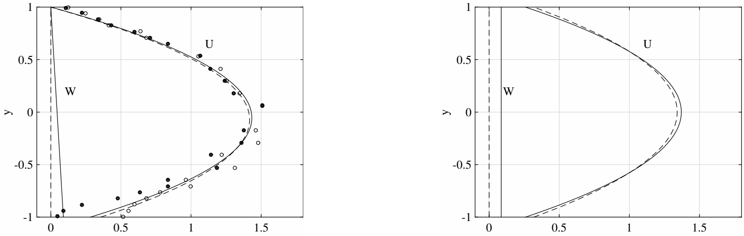

Figure: Streamwise U and spanwise W velocity components of the base flow when $\lambda^{\|} = 0.155$ for the cases $\theta = 0^\circ$ (dashed) and $\theta = 45^\circ$ (solid). Left: one superhydrophobic wall, Right: two superhydrophobic walls. The symbols show the experimental data from Ou and Rothstein (2005).

Linear stability analysis

We introduce a flow decomposition

$$\mathbf{u}(x, y, z, t) = (U, 0, W)(y) + \epsilon\tilde{\mathbf{u}}(y, t)\exp[i(\alpha\, x + \beta\, z)] + \text{c.c.}$$

where α and β are the streamwise and spanwise wavenumbers.

The linear equations are obtained collecting terms of order ϵ.

For the case of **two** superhydrophobic walls the boundary conditions read

$$\begin{bmatrix} \tilde{u}(\mp 1, t) \\ \tilde{w}(\mp 1, t) \end{bmatrix} = \pm \boldsymbol{\Lambda} \frac{\partial}{\partial y} \begin{bmatrix} \tilde{u}(\mp 1, t) \\ \tilde{w}(\mp 1, t) \end{bmatrix} \quad \text{and} \quad \tilde{v}(\mp, t) = 0$$

In the case of **one** superhydrophobic wall, at $y = -1$ the boundary conditions at $y = 1$ read

$$\tilde{\mathbf{u}}(1, t) = 0$$

Note: the theory is applicable if the wavelength is sufficiently longer than the spatial periodicity of the ridges.

Modal analysis

Here we assume a temporal behaviour such that

$$\tilde{\mathbf{u}}(y,t) = \hat{\mathbf{u}}(y)\exp(-i\,\omega\,t),$$

where ω is the complex angular frequency and $\omega_i > 0$ denotes unstable solutions.

On discrete form the resulting system of equations can be written

$$i\omega\mathbf{B}\hat{\mathbf{q}} = \mathbf{A}\hat{\mathbf{q}}, \tag{4}$$

where $\hat{\mathbf{q}} = (\hat{u}, \hat{v}, \hat{w}, \hat{p})$.

Spatial derivatives are discretized using second-order finite differences and the least stable eigenvalue is solved iteratively.

Results I

The onset of the instability is studied parametrically by varying the parameters $Re, \alpha, \beta, \lambda^{\parallel}$ and θ. We define the **critical Reynolds number** as

$$Re_c(\lambda^{\parallel}, \theta) = \min_{\alpha,\beta} Re(\alpha, \beta, \lambda^{\parallel}, \theta)$$

Two superhydrophobic walls

Dependency on Re_c by the ridge angle θ.

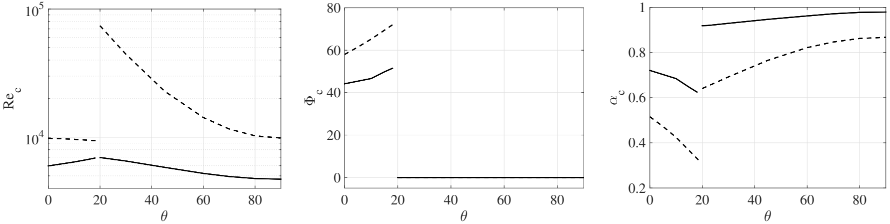

Figure: Critical Reynolds number Re_c (left) and corresponding wave angle (middle) and streamwise wavenumber (right) as a function of θ for the case of $\lambda^{\parallel} = 0.02$ **(−)** and $\lambda^{\parallel} = 0.05$ **(−−)** in the presence of two superhydrophobic walls. For no-slip $Re_c = 3848$.

Results II

Two superhydrophobic walls

Dependency on Re_c by slip length $\lambda^{\parallel}$.

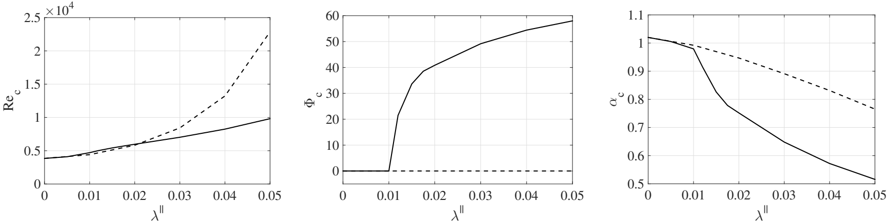

Figure: Critical Reynolds number Re_c (left) and corresponding wave angle (middle) and streamwise wavenumber (right) as a function of $\lambda^{\parallel}$ for the case of $\theta = 0$ **(−)** and $\theta = 45$ **(−−)** in the presence of two superhydrophobic walls. For no-slip $Re_c = 3848$.

Results III

One superhydrophobic wall

Dependency on Re_c by the ridge angle θ.

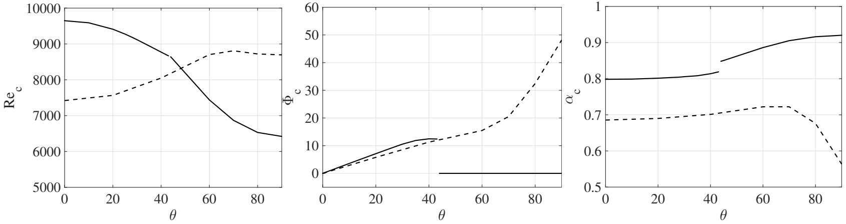

Figure: Critical Reynolds number Re_c (left) and corresponding wave angle (middle) and streamwise wavenumber (right) as a function of θ for the case of $\lambda^{\parallel} = 0.07$ **($-$)** and $\lambda^{\parallel} = 0.1553$ **($--$)** in the presence of one superhydrophobic wall. For no-slip $Re_c = 3848$.

Results IV

One superhydrophobic wall

Dependency on Re_c by slip length $\lambda^{\parallel}$.

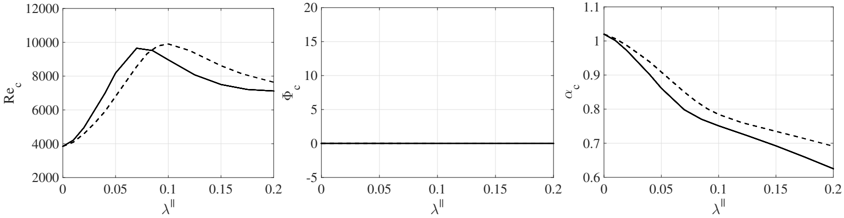

Figure: Critical Reynolds number Re_c (left) and corresponding wave angle (middle) and streamwise wavenumber (right) as a function of $\lambda^{\parallel}$ for the case of $\theta = 0$ **($-$)** and $\theta = 45$ **($--$)** in the presence of one superhydrophobic wall. For no-slip $Re_c = 3848$.

Nonmodal analysis

The non-modal behaviour is studied by computing the maximum finite-time amplification as a function of the parameters $Re, \alpha, \beta, \lambda^{\|}, \theta$ and T.

This is accomplished by computing the gain

$$G(Re, \alpha, \beta, T, \lambda^{\|}, \theta) = \max_{\tilde{\mathbf{u}}_0} \frac{e(T)}{e(0)} \tag{5}$$

where

$$e(t) = \frac{1}{2} \int_{-1}^{1} (\tilde{u}\tilde{u}^* + \tilde{v}\tilde{v}^* + \tilde{w}\tilde{w}^*) dy.$$

We further define the maximum gain as

$$G_M(Re, \lambda^{\|}, \theta) = \max_{\alpha, \beta, T} G$$

The problem is solved using an adjoint-based optimisation approach.

Results

Two superhydrophobic walls

Dependency on slip length $\lambda^{\parallel}$.

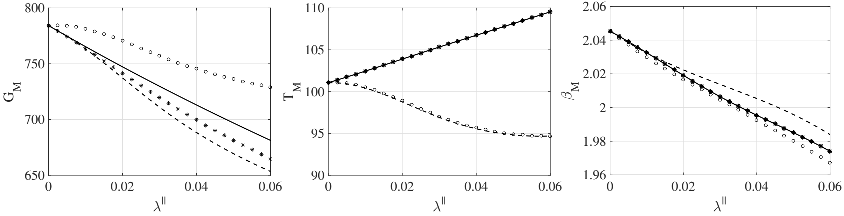

Figure: Gain G_M (left), corresponding time T_M (middle) and spanwise wavenumber β_M (right) as a function of $\lambda^{\parallel}$ in the case of $\theta = 0$ ($-$), $\theta = 15$ ($\star$), $\theta = 30$ ($--$), $\theta = 60$ ($\circ$), all for $Re = 1333$ and two superhydrophobic walls. In all cases the corresponding streamwise wave number $\alpha_M = 0$.

The above results are similar to those by Min and Kim (2005), when $\theta = 0$.

One superhydrophobic wall: ongoing work.

Classical optimal perturbation analysis

Initial streamwise vortices induce δU streaks

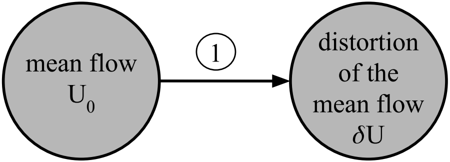

NO CYCLE

Self-sustained cycle

Wave-Vortex interaction

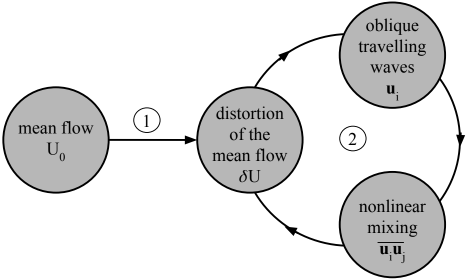

Hall & Smith (1991); Waleffe (1997); Hall & Sherwin (2010)

Weakly nonlinear analysis I

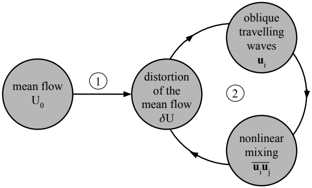

We decompose the velocity and pressure into a steady, laminar parallel state, a travelling wave and a slowly varying time-dependent base flow distortion. The optimization is based on the work by Biau and Bottaro (2009).

$$\begin{bmatrix} U_0(y) \\ 0 \\ W_0(y) \\ P_0(x) \end{bmatrix} + \epsilon \begin{bmatrix} u(x,y,z,t) \\ v(x,y,z,t) \\ w(x,y,z,t) \\ p(x,y,z,t) \end{bmatrix} + \epsilon^2 \begin{bmatrix} U(y,t) \\ V(y,t) \\ W(y,t) \\ P(y,t) \end{bmatrix}, \qquad (6)$$

where $\epsilon \in \mathbb{R}$ denotes the wave amplitude.

The disturbance at order $\mathcal{O}(\epsilon)$ is expressed using a single-mode Fourier decomposition in the streamwise and spanwise directions as

$$(\mathbf{u}, p)(x,y,z,t) = (\tilde{\mathbf{u}}, \tilde{p})(y,t)e^{i(\alpha x + \beta z)} + (\tilde{\mathbf{u}}^*, \tilde{p}^*)(y,t)e^{-i(\alpha x + \beta z)}. \qquad (7)$$

Weakly nonlinear analysis II

The governing equations, linearized around the perturbed base flow are given by

$$
\begin{aligned}
i\alpha\tilde{u} + \tilde{v}_y + i\beta\tilde{w} &= 0, && (8)\\
\tilde{u}_t + i\alpha(\mathbf{U_0} + \epsilon^{\mathbf{2}}\,\mathbf{U})\tilde{u} + \tilde{v}(\mathbf{U_0} + \epsilon^{\mathbf{2}}\,\mathbf{U})_y + i\beta(\mathbf{W_0} + \epsilon^{\mathbf{2}}\,\mathbf{W})\tilde{u} + i\alpha\tilde{p} &= \frac{1}{Re}\Delta_k\tilde{u}, && (9)\\
\tilde{v}_t + i\alpha(\mathbf{U_0} + \epsilon^{\mathbf{2}}\,\mathbf{U})\tilde{v} + i\beta(\mathbf{W_0} + \epsilon^{\mathbf{2}}\,\mathbf{W})\tilde{v} + \tilde{p}_y &= \frac{1}{Re}\Delta_k\tilde{v}, && (10)\\
\tilde{w}_t + i\alpha(\mathbf{U_0} + \epsilon^{\mathbf{2}}\,\mathbf{U})\tilde{w} + \tilde{v}(\mathbf{W_0} + \epsilon^{\mathbf{2}}\,\mathbf{W})_y + i\beta(\mathbf{W_0} + \epsilon^{\mathbf{2}}\,\mathbf{W})\tilde{w} + i\beta\tilde{p} &= \frac{1}{Re}\Delta_k\tilde{w}. && (11)
\end{aligned}
$$

At order $\mathcal{O}(\epsilon^2)$ the streamwise- and spanwise-averaged equations read

$$
\begin{aligned}
V &= 0, && (12)\\
U_t - \frac{1}{Re}U_{yy} &= -[\mathbf{\tilde{v}\tilde{u}_y^*} + \mathbf{\tilde{v}^*\tilde{u}_y} + \mathbf{i}\beta(\mathbf{\tilde{w}^*\tilde{u}} - \mathbf{\tilde{w}\tilde{u}^*})], && (13)\\
P_y &= -[\mathbf{i}\alpha(\mathbf{\tilde{u}^*\tilde{v}} - \mathbf{\tilde{u}\tilde{v}^*}) + \mathbf{\tilde{v}\tilde{v}_y^*} + \mathbf{\tilde{v}^*\tilde{v}_y} + \mathbf{i}\beta(\mathbf{\tilde{w}^*\tilde{v}} - \mathbf{\tilde{w}\tilde{v}^*})], && (14)\\
W_t - \frac{1}{Re}W_{yy} &= -[\mathbf{i}\alpha(\mathbf{\tilde{u}^*\tilde{w}} - \mathbf{\tilde{u}\tilde{w}^*}) + \mathbf{\tilde{v}\tilde{w}_y^*} + \mathbf{\tilde{v}^*\tilde{w}_y}]. && (15)
\end{aligned}
$$

Solution procedure

For assigned ϵ the nonlinear problem is solved iteratively in the following manner:

1. Maximise the energy $e(T)$ over a given time span T, to find $\tilde{u}, \tilde{v}, \tilde{w}$. The optimization procedure is performed via adjoint looping; in the first iteration $U = 0 \ \forall y, t$.
2. Solve for $U(y, t)$ and $W(y, t)$ under the initial condition $U(y, 0) = W(y, t) = 0$. Then, go back to (1).
3. Convergence is declared when the final wave energy $e(T)$ converges to within a defined precision. The normalization employed is $e(0) = \epsilon^2$.

Example I

$Re = 1333$, $\alpha = 0.085$, $\beta = 2.3$, different values of ϵ (no-slip)
In the equations we set $U_{BF} = U_0 + \epsilon^2 U$, $W_{BF} = W_0$

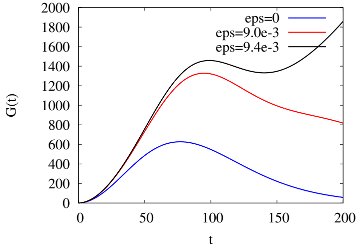

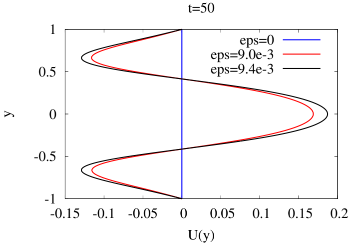

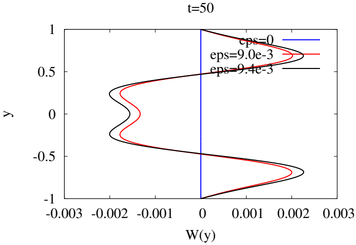

Example II

$Re = 1333$, $\alpha = 0.085$, $\beta = 2.3$, $\epsilon = 9.4 \times 10^{-3}$ (no-slip)
Comparison: $U_{BF} = U_0 + \epsilon^2 U$, $W_{BF} = W_0$ vs $U_{BF} = U_0 + \epsilon^2 U$, $W_{BF} = W_0 + \epsilon^2 W$

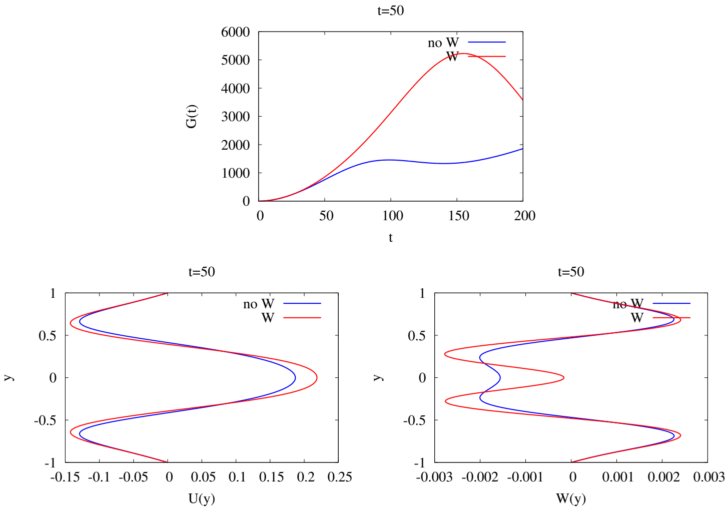

Couette flow

To set ideas let us consider no slip walls.

Linear optimal disturbances over a short time frame

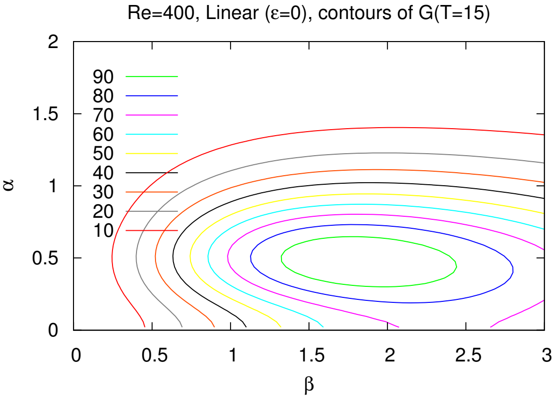

$$\alpha_{opt} = 0.475,\ \beta_{opt} = 1.81,\ G_{max} = 99.4$$

$$(G_{max \forall T} = 188.8 \text{ @ } T_{max} = 46.8,\ \alpha = 0.0875,\ \beta = 1.6)$$

What happens when the amplitude increases?

Results for linear optimal parameters obtained at $T = 15$, for ϵ increasing and varying T

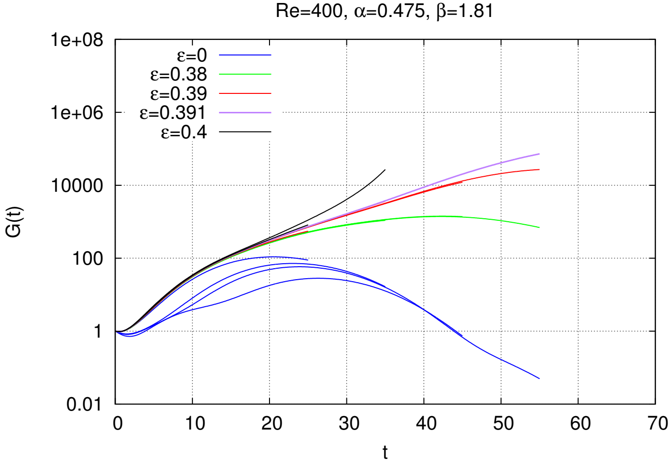

Beyond $\epsilon = 0.391$ the gain explodes

Mean flow distortion

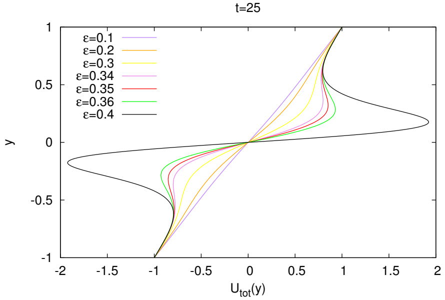

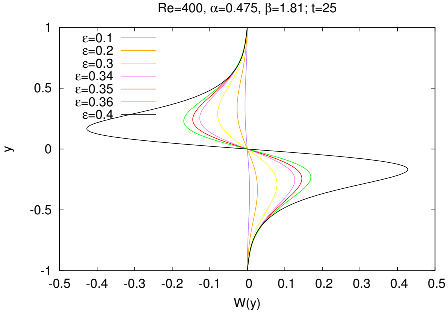

Deformation built up by Reynolds stresses

Disturbance waves

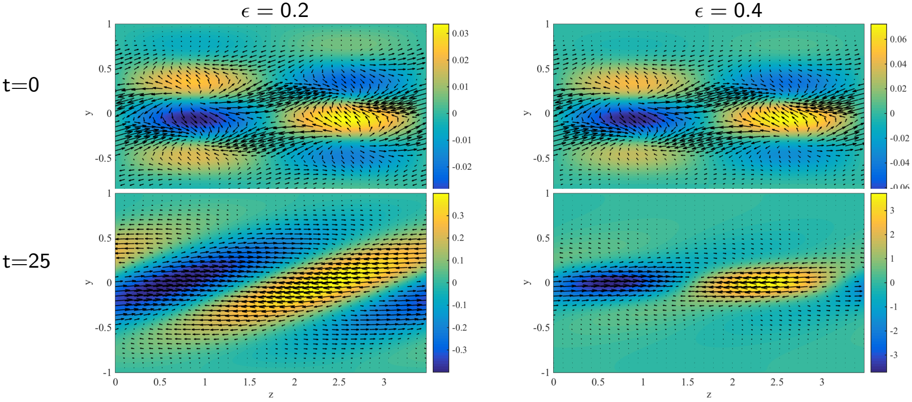

Contours of streamwise perturbation velocity and vectors of cross-stream components

Nonlinear optimals

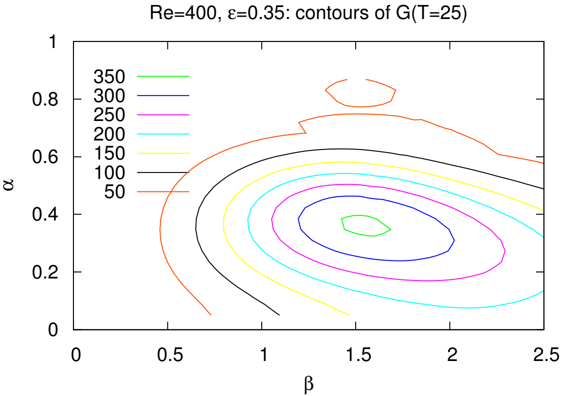

$$\alpha_{opt} = 0.35, \ \beta_{opt} = 1.55$$

Nonlinear optimals

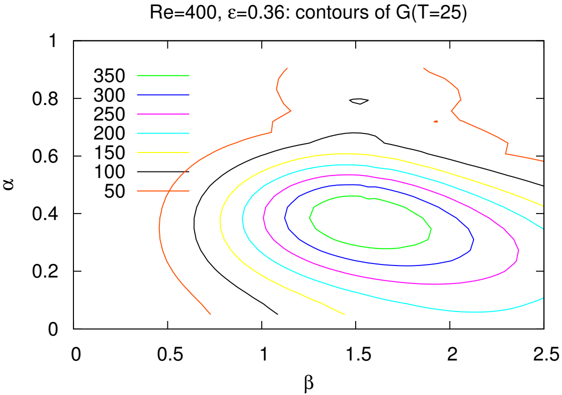

Nonlinear optimals

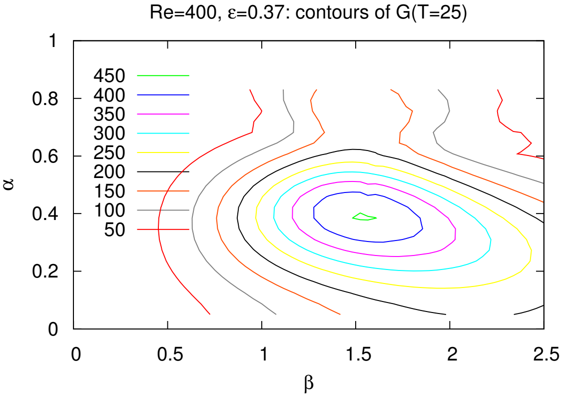

Nonlinear optimals

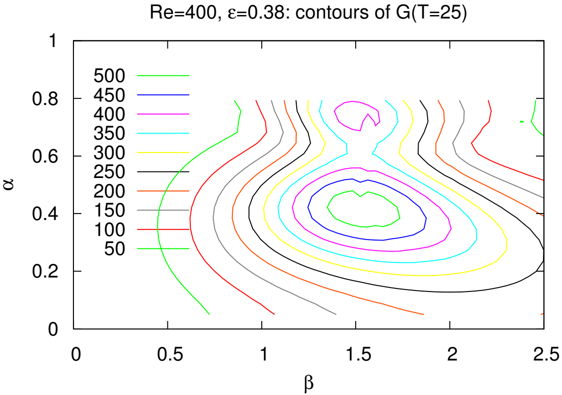

Nonlinear optimals

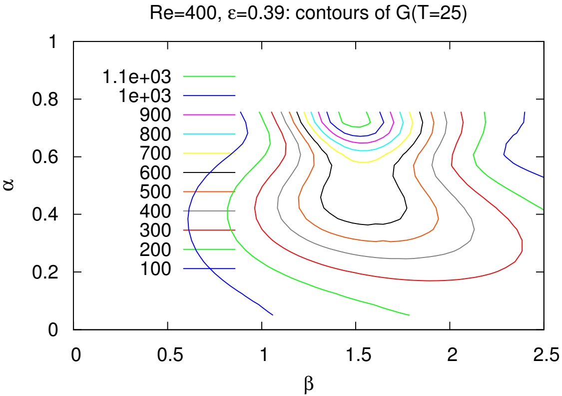

$$\alpha_{opt} = 0.74, \ \beta_{opt} = 1.5$$

Varying T

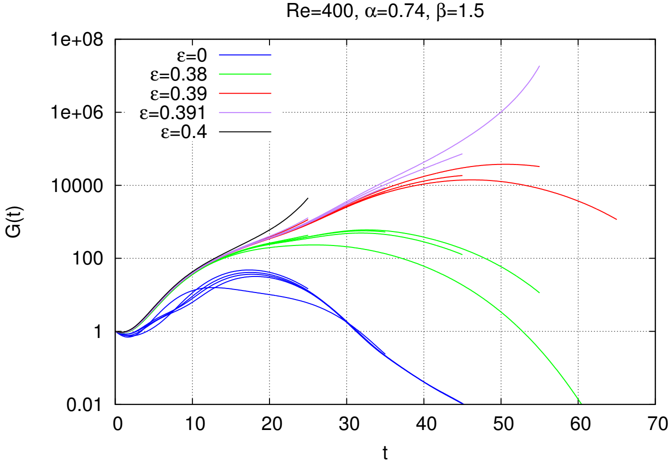

Beyond $\epsilon = 0.39$ the gain explodes

Conclusions

- A **linear** and **weakly nonlinear** analysis of the flow in a channel has been conducted
- We have studied surface topography constituted by micro-ridges with **arbitrary alignment**.
- The results of the linear nonmodal study **complete** those by Min and Kim (2005) by varying $\lambda^{\parallel}$ and θ.
- Both modal and nonmodal analysis show that instability onset is **delayed** applying a superhydrophobic surface (both one- and two-sided) in a plane channel.
- Nonlinear results will permit to identify **threshold amplitudes** of disturbances provoking transition (for the flow in a micro-channel bound by one or two superhydrophobic surfaces).

References I

M. Z. Bazant and O. I. Vinogradova. Tensorial hydrodynamic slip. *J. Fluid Mech.*, 613:125–134, 2008.

A. V. Belyaev and O. I. Vinogradova. Effective slip in pressure-driven flow past super-hydrophobic stripes. *J. Fluid Mech.*, 652:489–499, 2010.

D. Biau and A. Bottaro. An optimal path to transition in a duct. *Phil. Trans. R. Soc. A*, 367: 529–544, 2009.

E. Lauga and H. A. Stone. Effective slip in pressure-driven Stokes flow. *J. Fluid Mech.*, 489: 55–77, 2003.

T. Min and J. Kim. Effects of hydrophobic surface on stability and transition. *Phys. Fluids*, 17: 108106, 2005.

J. Ou and J. P. Rothstein. Direct velocity measurements of the flow past drag-reducing ultrahydrophobic surfaces. *Phys. Fluids*, 17:103606, 2005.

J. R. Philip. Flows satisfying mixed no-slip and no-shear conditions. *Z. Andew. Math. Phys.*, 23: 353–370, 1972.